

Delayed melting at the substrate interface of amorphous Ge films partially melted with nanosecond laser pulses

F. Vega^{a)}

Department d'Optica i Optometria (Universitat Politècnica de Catalunya), C/Violinista Vellsola 37 08222-Terrassa, Spain

J. Solis, J. Siegel, and C. N. Afonso^{b)}

Instituto de Optica del CSIC, C/Serrano 121 28006-Madrid, Spain

(Received 6 April 2000; accepted for publication 30 August 2000)

The dynamics of melting-rapid solidification of amorphous Ge films on transparent substrates upon irradiation with nanosecond laser pulses has been analyzed by means of real time reflectivity measurements performed both at the air-film and film-substrate interfaces. The effect of the heat flow conditions on the rapid solidification process has been studied by comparing the behavior of films with thicknesses ranging from 50 to 180 nm on substrates with different thermal conductivities like glass, quartz, and sapphire. The films deposited onto substrates of low thermal conductivity (glass and quartz) undergo a local delayed melting process in the vicinity of the film-substrate interface, the process being dependent on the film thickness and/or the laser fluence. This delayed melting process is never observed in films deposited on sapphire. The comparison of the results suggests that the solidification heat released from the primary melt is responsible for the delayed melting process at the film-substrate interface whenever the heat-transfer ratio to the substrate is low enough. © 2000 American Institute of Physics. [S0021-8979(00)05423-2]

INTRODUCTION

Excimer pulsed laser processing of amorphous semiconductors is currently applied to obtain polycrystalline thin films on insulating substrates.^{1,2} Although most of the work reported has been carried out in Si films^{3,4} there is an increasing interest in the study of laser crystallization of amorphous Ge(*a*-Ge) films because of their potential application to the fabrication of infrared detectors as well as substrates for GaAs solar cells due to the low mismatch between the two lattice parameters. The crystallization process involves primarily the melting of the *a*-Ge film followed by its rapid solidification. It has been pointed out^{5,6} that the ability of inducing very near surface melting without appreciable heating of the substrate is a key point in order to make this technique compatible with low cost substrates. Nevertheless, these substrates are usually poor heat conductors and thus the heat transfer to the substrate can be slowed down leading to substantially different solidification processes.⁷

The use of real time reflectivity (RTR) measurements at the film surface is a well established technique to monitor the laser induced melting-rapid solidification process. However, once the metallic liquid phase is formed at the film surface, the optical penetration depth becomes very small (a few nanometers) and the reflectivity measurements performed at the film surface are unable to provide in-depth information about the process dynamics. To overcome this problem, the reflectivity measurements have been combined with transient conductance measurements,⁸⁻¹⁰ but this technique requires a complex patterning of the films to form the metallic contacts.

When dealing with transparent substrates, a simpler alternative is to perform RTR measurements at both the front and back film surfaces, the latter meaning to monitor the reflectivity variations at the film-substrate interface through the substrate. Although this kind of measurement provides very sensitive time and in-depth information of the structural state of the film,^{7,11,12} it has scarcely been used.

The aim of this work is to study by means of front and back surface reflectivity measurements the dynamics of rapid solidification of *a*-Ge films melted by UV nanosecond laser pulses. Special attention is paid to the role of the heat flow transfer to the substrate by comparing the behavior of films with thicknesses ranging from 50 to 180 nm on substrates with increasing thermal conductivities such as glass, quartz, and sapphire. Upon partial melting of the films deposited onto substrates of low thermal conductivity (glass and quartz), the back surface RTR measurements show a delayed melting process located near the substrate boundary. This process can even occur after the complete solidification of the primary melted material and it is never observed in films deposited on sapphire that is the substrate with the higher thermal conductivity.

EXPERIMENT

The Ge films are grown at room temperature in a dc magnetron sputtering system onto glass, quartz, and sapphire. These substrates have increasing room-temperature thermal conductivities $k = 2.8 \times 10^{-3}$ W/K cm, 5.8×10^{-3} W/K cm, and 66.4×10^{-3} W/K cm, respectively.¹³⁻¹⁶ The as-deposited films have thicknesses of 50, 100, and 180 nm and are amorphous, homogeneous, and dense with a low fraction of voids.¹⁷ The films are irradiated in air by single ArF laser

^{a)}Electronic mail: fvega@oo.upc.es

^{b)}Electronic mail: cnafonso@io.cfmac.csic.es

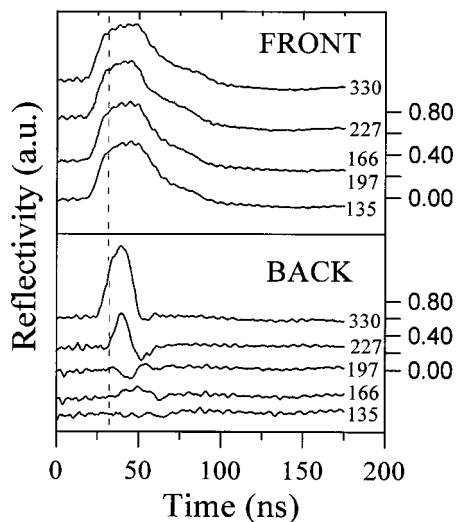


FIG. 1. Front and back RTR transients obtained in a 180 nm *a*-Ge film on sapphire. The transients have been vertically shifted for the sake of clarity but preserving their relative scales. For a given transient, the vertical distance between two points can be converted to a reflectivity difference by using the scale included in the right vertical axis. The laser fluence used for each transient is given in mJ/cm^2 on its right. The vertical dashed line indicates the temporal location of the maximum of the irradiation laser pulse.

pulses ($\lambda = 193 \text{ nm}$, $\tau = 12 \text{ ns}$) impinging the air-film interface at normal incidence. A beam homogenizer has been used to obtain an homogeneous beam profile at the sample site with constant fluence (within 5%) over a square region of $4 \times 4 \text{ mm}^2$. The evolution of the film reflectivity has been monitored by means of a HeNe laser at both the air-film and the film-substrate interfaces that will be referred to from now on as front and back reflectivities. The He-Ne laser ($\lambda = 633 \text{ nm}$), pulsed to $\tau = 1 \mu\text{s}$ by means of an acousto-optic modulator, is focused at the center of the irradiated area. The experimental configuration for both the pump and probe beams is similar to that reported elsewhere.⁷ The detection system is formed by a fast photodiode connected to a digitizer, the time resolution of the reflectivity measurements being a few nanoseconds. Each area is irradiated only once and for a given fluence value, at least one front and one back RTR transient are recorded. Further details about the irradiation and detection setup can be found elsewhere.¹⁸

RESULTS

Since the *a*-Ge films are deposited on different substrates and have different thickness, they have a different initial reflectivity. To ease the comparison of the results, all the reflectivity changes will be given as $(R_t - R_0)/R_0$, where R_t is the reflectivity at instant t and R_0 is the initial film reflectivity. Figure 1 shows both front and back RTR transients obtained at increasing laser fluences in the 180 nm *a*-Ge film on sapphire. Similar results have been obtained in the 50- and 100-nm-thick *a*-Ge films on sapphire. For each front RTR transient we have plotted the corresponding back RTR transient obtained with the same fluence. Since all the transients are plotted in the same vertical scale but vertically shifted, the RTR transients in Fig. 1 allow us to follow si-

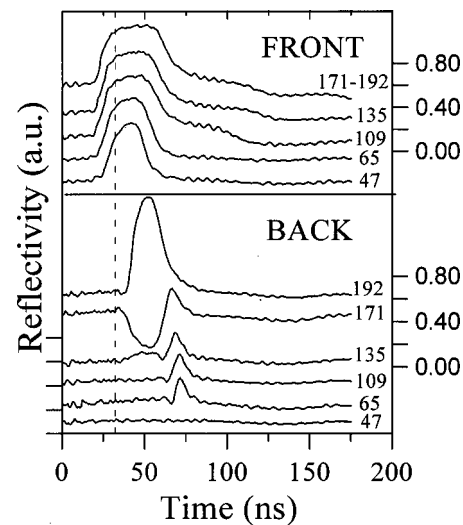


FIG. 2. Front and back RTR transients obtained in a 180 nm *a*-Ge film on glass. The laser fluence used for each transient is given in mJ/cm^2 on its right. The transients have been vertically shifted for the sake of clarity but preserving their relative scales. For a given transient, the vertical distance between two points can be converted to a reflectivity difference by using the scale included in the right vertical axis. The vertical dashed line indicates the temporal location of the maximum of the irradiation laser pulse.

multaneously the laser induced melting and solidification processes as seen from both the air-film and film-substrate interfaces. For the lowest fluence shown ($135 \text{ mJ}/\text{cm}^2$), the front RTR transient shows the features widely reported upon laser induced melting and solidification of semiconductors.¹⁹⁻²¹ A reflectivity increase up to a maximum level related to the formation of a metallic liquid layer at the surface followed by a decrease related to the solidification and cooling processes. The shape of all the front RTR transients is essentially the same and all of them exhibit a *shoulder* in the cooling tail which is generated by a process usually referred to as *recalescence*. This process has thoroughly been described by several authors²²⁻²⁶ and is related to an increase of temperature of the melt due to the release of the solidification enthalpy upon nucleation of the solid phase. It has earlier been demonstrated that a minimum melt depth and thus a minimum amount of initially solidified material is necessary to observe recalescence effects.^{7,23,24} Moreover, it has been extensively shown that the occurrence of recalescence involves the resolidification of the material in the polycrystalline phase or as mixture of amorphous and polycrystalline material regardless of both the film thickness and the choice of the substrate.^{21,25-27}

The back RTR transients recorded at fluences up to $135 \text{ mJ}/\text{cm}^2$ are flat, thus indicating that the primary melt front does not progress deep enough to be detected at the backside. The transient obtained at $166 \text{ mJ}/\text{cm}^2$ shows a small reflectivity maximum whereas for higher fluences either a minimum (transient recorded at $197 \text{ mJ}/\text{cm}^2$) or a clear maximum (transient obtained at $227 \text{ mJ}/\text{cm}^2$) can be observed. It is worth noting that the reflectivity change at the maximum increases with the laser fluence up to a value of ≈ 0.80 (transient measured at $330 \text{ mJ}/\text{cm}^2$).

Figure 2 shows both front and back RTR transients obtained at increasing laser fluences in the 180 nm *a*-Ge film

on glass. Similar results have been obtained in the 50- and 100-nm-thick films on quartz. As in the case of the *a*-Ge film on sapphire, the front RTR measurements show that the film surface is melted upon laser irradiation for the lowest fluence shown (47 mJ/cm^2). For fluences above 109 mJ/cm^2 , the recalescence process is clearly observed in the decreasing tail of the transients. The shape and features of the front RTR transients for fluences between the recalescence threshold and the maximum fluence studied ($\approx 200 \text{ mJ/cm}^2$) are essentially the same.

The back RTR transients are featureless at the lowest fluence studied (47 mJ/cm^2). For fluences in the range 65 – 171 mJ/cm^2 , a new feature can be appreciated that is never observed in *a*-Ge films deposited on sapphire: a reflectivity maximum (that will be referred to as the *delayed peak*) delayed with respect to the cooling tail of the corresponding front RTR transient. By measuring the reflectivity value at the front transient when the delayed peak occurs in the corresponding back transient, and comparing this value with the reflectivity of liquid Ge(*l*-Ge), it can be concluded that when the delayed peak occurs in the back transients the melted layer at the front surface has resolidified either completely (in absence of recalescence) or nearly completely (if recalescence is present, transients obtained between 109 and 171 mJ/cm^2). The reflectivity at the delayed peak is nearly insensitive to the fluence and its maximum value corresponds to a reflectivity change close to 0.20 . It is also worth noting that this peak can be preceded either by a slight reflectivity increase (back RTR transient recorded at 135 mJ/cm^2) or a clear minimum for higher fluences (back RTR transient recorded at 171 mJ/cm^2). Finally, for the highest fluence used (transient obtained at 192 mJ/cm^2), the back RTR transient shape is similar to that of the front one in the sense that it shows a single maximum with a reflectivity change of ≈ 0.84 .

DISCUSSION

In order to correlate the time evolution of the reflectivity measured at the front and the back sides of the samples with the actual transformation depth, optical simulations of the induced reflectivity changes upon film melting and solidification have been performed by using a home developed computer program based on the theory of the optical properties of thin film multilayers.²⁸ The program calculates the reflectivity evolution both at the front and back film interfaces by transforming the optical constants of the as-deposited film (*a*-Ge) into the constants of liquid Ge(*l*-Ge). The calculations are done modifying layer by layer the film structure as a liquid-solid interface propagates in depth. The program also allows us to simulate the propagation of thin liquid buried layers. Figure 3 shows the calculated front and back reflectivity changes of *a*-Ge films on glass as a function of the melted thickness and when melting starts at the air-film interface. The complex refractive index used (*n-ik*) are $n_{a\text{-Ge}}=4.68$, $k_{a\text{-Ge}}=1.85$, $n_{l\text{-Ge}}=3.26$ and $k_{l\text{-Ge}}=5.92$.^{17,19} The refractive index used for the glass substrate is $n_{\text{glass}}=1.52$.²⁹ The oscillatory behavior of the reflectivity that is

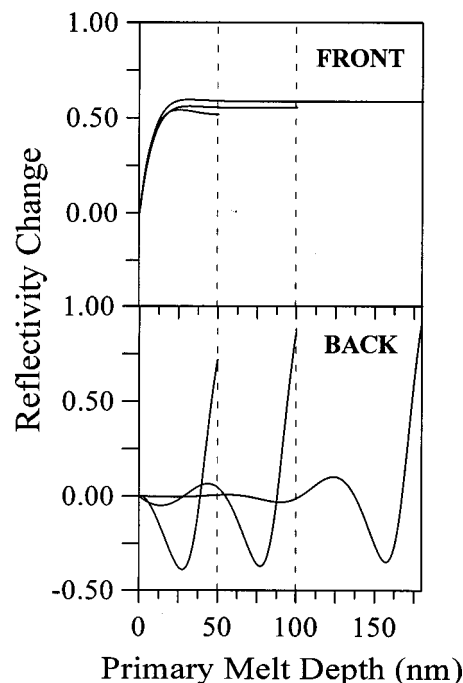


FIG. 3. Simulation of the changes in the front and back reflectivities at $\lambda = 633 \text{ nm}$ as a liquid Ge layer progresses in depth in a 50, 100, and 180 nm *a*-Ge film on glass.

observed in the simulation of the back reflectivity in Fig. 3, indicates the existence of optical interference effects as the melting front propagates toward the substrate.

In the case of films deposited on quartz or sapphire, the curves obtained are completely similar in the sense that the maxima and minima of reflectivity occur at the same primary melt depth although the particular value of the reflectivity change at these extremes depends on the refractive index of the substrate and thus are slightly different.

For the thickest film (180 nm), it is seen that the back-reflectivity probe will only be sensitive to variations of the primary melt depth once it is thicker than approximately 100 nm. Above this depth, the calculated reflectivity first increases slightly and undergoes a clear reflectivity minimum for a melt depth of $\approx 160 \text{ nm}$. A very sharp reflectivity increase that reaches a maximum of 0.91 occurs once the whole film is melted. A similar behavior is predicted for the 50-nm and 100-nm-thick *a*-Ge films, although it is clearly seen that the back reflectivity probe becomes sensitive to shallower melt depths as the film thickness decreases. Finally, Fig. 3 also shows that for *l*-Ge layers thicker than $\approx 15 \text{ nm}$ the front reflectivity probe becomes “saturated” and thus insensitive to thicker melt depths.

In the case of the transients recorded upon laser irradiation of the 180 nm *a*-Ge film on sapphire, the shape of the back RTR transients for fluences in the range 166 – 197 mJ/cm^2 (Fig. 1) is consistent with the variations of the reflectivity changes observed in the simulation when the melt front reaches a depth $\geq 100 \text{ nm}$ (see Fig. 3). Further support is given by the fact that these backreflectivity variations occur at times for which the front RTR transients exhibit the high reflectivity phase that corresponds to the primary *l*-Ge layer. It is thus possible to conclude that within this fluence

range, the melt front progresses far enough in depth as to be probed by the backreflectivity. Further increases of the laser fluence lead to nearly complete melting of the *a*-Ge film as evidenced by the similar high reflectivity phase seen in both the front and back RTR transients for the highest studied fluence (330 mJ/cm²).

The back RTR transients recorded upon laser irradiation of the *a*-Ge films on glass and quartz present a quite different behavior since the delayed peak is always observed. The reflectivity variations that precede the delayed peak (see Fig. 2, back RTR transients recorded in the fluence range 135–171 mJ/cm²) are similar to the ones calculated in the simulation when the melt front reaches a large depth (see Fig. 3). Moreover, these reflectivity variations occur at times for which the front RTR transients still exhibit the high reflectivity phase that corresponds to the primary *l*-Ge layer. Finally, and similarly to the case of the films deposited on sapphire, further increases of the laser fluence lead to nearly complete melting of the *a*-Ge film as evidenced by the high reflectivity change (0.84) at the maximum of the back RTR transients (see transient recorded at 192 mJ/cm² in Fig. 2) that corresponds to a ≈ 176 -nm-thick *l*-Ge layer according to the calculations included in Fig. 3.

The comparison of the back RTR transients to the reflectivity simulations in Fig. 3 allows us to determine the melt-in time and to estimate the maximum melt depth induced for a given fluence. In the case of the 180 nm *a*-Ge film on glass, the presence of a net reflectivity minimum (back RTR transient at 171 mJ/cm²) is consistent with a melt depth front reaching a depth of about 160 nm (Fig. 3) in approximately 20 ns (melt-in front velocity of 8 m/s). Since nearly the whole 180 nm film is melted at a fluence of 192 mJ/cm² (Fig. 2) and assuming, as widely reported, that the melt depth is directly proportional to the fluence,¹⁶ the calculated slope is about 0.95 (nm)/(mJ/cm²). Then, in the case of the back RTR transient recorded at 109 mJ/cm² in which no reflectivity variation before the delayed peak is observed, the estimated melt depth would be ≈ 75 nm,³⁰ i.e., below the minimum melt depth at which the back probe beam is sensitive to the initial melt front (Fig. 3). The same calculation for an intermediate fluence like 135 mJ/cm² for which some reflectivity variations before the delayed peak are seen, leads to a melt depth of ≈ 100 nm, i.e., around the minimum melt depth at which the back probe beam starts to be sensitive (Fig. 3). Such a good agreement between this simple calculation and the experimental results further confirms that the reflectivity variations that precede the delayed reflectivity peak are caused by the progress of the primary melt front. This reasoning also applies to the 100-nm-thick *a*-Ge films deposited on the lower thermal conductivity substrates. In the case of the thinnest films (50 nm) and because of both the temporal resolution of our detection system and the sensitivity of the back probe to shallow primary melt layers (Fig. 3), the delayed peak can hardly be resolved from the primary melt front.

The fact that the maximum of the delayed peak corresponds to a relatively large reflectivity change of ≈ 0.20 suggests that the observed delayed peak is most likely related to the presence of a very thin Ge liquid layer located in the

vicinity of the film-substrate interface since otherwise (with a moving front), the reflectivity first should decrease and undergo a minimum according to the calculations shown in Fig. 3. Furthermore, the calculations show that to achieve a reflectivity change of 0.20, it is just necessary a 2–3-nm-thick Ge liquid layer at the substrate interface.

To explain the origin of this thin Ge liquid layer at the substrate interface, we should consider that under similar conditions with an strongly undercooled primary liquid layer on top of a remnant nonmelted amorphous layer, the self-propagation of thin buried liquid layers through the amorphous material has been reported.^{31–33} This process occurs when the primary melt front resolidifies as crystalline material with a melting point higher than the one of the remnant amorphous phase. When the RTR measurements were used to monitor the propagation of the buried liquid layer, very characteristic maxima and minima of interference were seen in both the front^{34,35} and back reflectivity¹² signals. Since our front reflectivity transients do not exhibit such reflectivity oscillations, we can discard the propagation of a thin buried *l*-Ge layer as responsible for the appearance of the delayed reflectivity peak.

The results show that this delayed melting process at the film-substrate interface occurs once the primary *l*-Ge has resolidified (totally or partially) and thus, the solidification latent heat has been released through the remnant *a*-Ge layer to reach the glass or quartz substrates. It is well known that the heat flow rate in a material depends on both, its thermal conductivity and the local temperature gradient. Since the thermal conductivity of the substrates ($k_{\text{glass}} = 2.8 \times 10^{-3}$ and $k_{\text{quartz}} = 5.8 \times 10^{-3}$ W/K cm) are lower than the one of *a*-Ge ($k = 10^{-2}$ W/K cm),²⁴ and assuming that the local temperature gradient at the film-substrate interface is essentially the same in the *a*-Ge film and in the substrate side, a reduction of the heat flow rate by an amount of $k_{\text{substrate}}/k_{a\text{-Ge}}$ would occur at the film-substrate interface. This could give rise to a transient temperature increase large enough to induce local melting at the interface. Further support to this reasoning comes from the fact that the delayed peak is never observed when using a substrate like sapphire that exhibits a thermal conductivity ($k = 6.6 \times 10^{-2}$ W/K cm) higher than that of *a*-Ge. Actually, at the film-substrate interface one can expect a higher density of defects like voids which could locally reduce the melting point below that of *a*-Ge. Moreover, the stresses at the neighborhood of the film-substrate interface might also lead to local changes in the degree of relaxation which could lead to further local reduction of the melting point.^{21,36–38} All these reasons suggest that the delayed melting process is triggered by the heat released by the primary solidification front that is not efficiently released to the substrate due to its lower thermal conductivity. The reduction of the heat flow rate at the film-substrate interface induces local melting at temperatures below that of the “bulk” film material at defective/stressed sites in the vicinity of the film-substrate interface. An additional experimental result that supports this interpretation is the fact that the delayed peak has a maximum value that is nearly insensitive either to the laser fluence or to the primary melt depth. Even for melt depths for which a high amount of latent heat is released, the

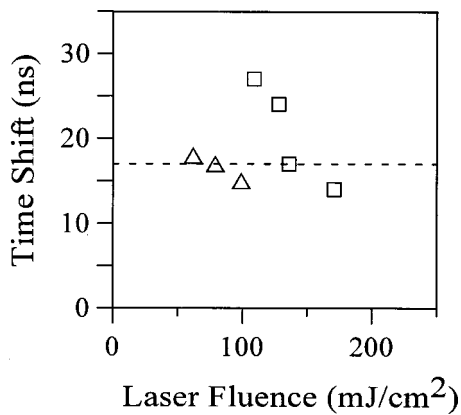


FIG. 4. Time shift of the delayed peak observed in the back RTR transients in respect to the time at which the primary melt front reaches its maximum depth as a function of the laser fluence for both the 100 (Δ) and 180 (\square) nm thick *a*-Ge films on glass. The dashed line corresponds to a constant time delay of 17 ns.

delayed melting process seems to be restricted to a thin region located at the film-substrate interface.

Finally, let us analyze in more detail the transfer of the solidification latent heat through the remnant nonmelted amorphous film to the substrate. In this context, it is clear that the deeper the primary melt front, the smaller the distance l that the released solidification heat should travel in order to reach the film-substrate interface and the faster the released heat arrives there. Consequently, the *time shift* between the time at which the primary melt front reaches its maximum penetration depth and the occurrence of the maximum of the delayed peak should decrease for increasing fluences. The results are plotted in Fig. 4 for both the 100-nm and 180-nm-thick *a*-Ge films on glass where it is clearly seen that they follow the expected trend. No results are included for the 50 nm *a*-Ge film since the delayed peak could hardly be resolved from the primary melt front as mentioned before. For a certain time shift, the distance l should be the same no matter the film thickness. We have calculated this distance for the two films and for a delayed peak position of 17 ns (shown as a dashed line in Fig. 4) and the result is of 57 ± 2 nm regardless of the film thickness.³⁹

The minimum time to transfer heat from the melt front through the remnant *a*-Ge to the substrate can be estimated as $t \approx l^2/4D$, where D stands for the thermal diffusivity of *a*-Ge.²⁴ The calculated values are in the 1 ns range, i.e., an order of magnitude smaller than the time shifts experimentally measured and plotted in Fig. 4. This result indicates, on one hand, that the heat released by the solidification front has enough time to reach the substrate. On the other hand, it shows that the delayed melting process at the substrate-film interface occurs once a considerable amount of heat reaches the interface and thus enough material has resolidified from the primary melt.

CONCLUSIONS

A delayed melting process most likely related to defective/stressed regions in the vicinity of the film-substrate interface has been identified by means of back RTR mea-

surements. This process occurs at the film-substrate interface, once the primary melt front has solidified (partially or completely) and the solidification enthalpy reaches the film-substrate interface. Since the delayed melting process has never been observed in *a*-Ge films on substrates of high thermal conductivity such as sapphire, this effect is most likely related to the reduction of the heat transfer rate at the boundary of substrates with a thermal conductivity lower than that of the film, like glass or quartz.

ACKNOWLEDGMENT

The Marie Curie TMR program for the European Union (ERB40001GT54352) is acknowledged for financial support.

- ¹J. S. Im and H. J. Kim, Appl. Phys. Lett. **64**, 2303 (1994).
- ²H. Kuriyana, T. Nohda, Y. Aya, T. Kuwahara, K. Wakisaka, S. Kiyama, and S. Tsuda, Jpn. J. Appl. Phys., Part 1 **33**, 5657 (1994).
- ³D. Toet, B. Koopmans, P. V. Santos, R. B. Bergmann, and B. Richards, Appl. Phys. Lett. **69**, 3719 (1996).
- ⁴G. K. Giust and T. W. Sigmon, J. Appl. Phys. **81**, 1204 (1997).
- ⁵M. Mulato, D. Toet, G. Aichmair, P. V. Santos, and I. Chambouleyron, J. Appl. Phys. **82**, 5158 (1997).
- ⁶L. Mariucci *et al.*, Thin Solid Films **337**, 137 (1999).
- ⁷J. Siegel, J. Solis, and C. N. Afonso, J. Appl. Phys. **84**, 5531 (1998).
- ⁸G. J. Galvin, M. O. Thompson, J. W. Mayer, R. B. Hammond, N. Paulter, and P. S. Peercy, Phys. Rev. Lett. **48**, 33 (1982).
- ⁹S. R. Stiffler, M. O. Thompson, and P. S. Peercy, Phys. Rev. Lett. **60**, 2519 (1988).
- ¹⁰S. R. Stiffler, M. O. Thompson, and P. S. Peercy, Phys. Rev. B **43**, 9851 (1991).
- ¹¹J. Boneberg, J. Nedelcu, H. Bender, and P. Leiderer, Mater. Sci. Eng., A **173**, 347 (1993).
- ¹²K. Murakami, O. Eryu, K. Takita, and K. Masuda, Phys. Rev. Lett. **59**, 2203 (1987).
- ¹³J. Solis and C. N. Afonso, J. Appl. Phys. **72**, 2125 (1992).
- ¹⁴E. Fogarassy, B. Prevot, S. De Unamuno, M. Elliq, H. Pattyn, E. L. Mathe, and A. Naudon, Appl. Phys. A: Solids Surf. **56**, 365 (1993).
- ¹⁵A. Jadin, I. V. Filiouguine, M. Wautelet, and L. D. Laude, Appl. Surf. Sci. **46**, 375 (1990).
- ¹⁶M. O. Thompson, G. J. Galvin, J. W. Mayer, P. S. Peercy, and R. B. Hamond, Appl. Phys. Lett. **42**, 445 (1983).
- ¹⁷J. G. de Sande, C. N. Afonso, J. L. Escudero, R. Serna, F. Catalina, and E. Bernabeu, Appl. Opt. **31**, 6133 (1992).
- ¹⁸J. Solis, F. Vega, and C. N. Afonso, Appl. Phys. A: Mater. Sci. Process. **62**, 197 (1996).
- ¹⁹G. E. Jellison, Jr., D. H. Lowndes, D. N. Mashburn, and R. F. Wood, Phys. Rev. B **34**, 2407 (1986).
- ²⁰J. Solis and C. N. Afonso, J. Appl. Phys. **69**, 2105 (1991).
- ²¹F. Vega, R. Serna, C. N. Afonso, D. Bermejo, and G. Tejada, J. Appl. Phys. **75**, 7287 (1994).
- ²²S. R. Stiffler, M. O. Thompson, and P. S. Peercy, Appl. Phys. Lett. **56**, 1025 (1990).
- ²³T. Sameshima and S. Usui, J. Appl. Phys. **74**, 6592 (1993).
- ²⁴F. Vega, C. N. Afonso, W. Szyszko, and J. Solis, J. Appl. Phys. **82**, 2247 (1997).
- ²⁵J. Siegel, J. Solis, C. N. Afonso, and C. García, J. Appl. Phys. **80**, 6677 (1996).
- ²⁶J. Siegel, J. Solis, and C. N. Afonso, Appl. Phys. Lett. **75**, 1071 (1999).
- ²⁷C. N. Afonso, J. Solis, F. Vega, J. Siegel, and W. Szyszko, Appl. Surf. Sci. **109/110**, 20 (1997).
- ²⁸H. A. Macleod, *Thin Film Optical Filters*, 2nd ed. (Hilger, London, 1986).
- ²⁹E. D. Palik, *Handbook of Optical Constants of Solids* (Academic, New York, 1985).
- ³⁰The melt depth is estimated from the formula: $m \times (F - E_{th})$, where $m = 0.95$ (nm)/(mJ/cm²) is the calculated slope for the dependence of the melt depth on fluence, F in mJ/cm² is the fluence and $E_{th} = 30$ mJ/cm² is the experimentally determined melting threshold.
- ³¹M. O. Thompson, G. J. Galven, J. W. Mayer, P. S. Peercy, J. M. Poate, D. C. Jacobson, A. G. Cullis, and N. G. Chew, Phys. Rev. Lett. **52**, 2360 (1984).

- ³²W. Sinke and F. W. Saris, Phys. Rev. Lett. **53**, 2121 (1984).
- ³³R. F. Wood and G. A. Geist, Phys. Rev. Lett. **57**, 873 (1986).
- ³⁴D. H. Lowndes, G. E. Jellison, Jr., S. J. Pennycook, S. P. Withrow, and D. N. Mashburn, Appl. Phys. Lett. **48**, 1389 (1986).
- ³⁵J. J. P. Bruines, R. P. M. van Hal, H. M. J. Boots, A. Polman, and F. W. Saris, Appl. Phys. Lett. **49**, 1160 (1986).
- ³⁶W. C. Sinke, S. Roorda, and F. W. Saris, J. Mater. Res. **3**, 1201 (1998).
- ³⁷M. G. Grimaldi and P. Baeri, Appl. Phys. Lett. **57**, 614 (1990).
- ³⁸J. Solis, J. Siegel, C. N. Afonso, J. Jimenez, and C. García, J. Appl. Phys. **82**, 236 (1997).
- ³⁹The distance l is calculated from the formula $[m' \times (F - E_{th}) \times t]$, where $m' = 0.05$ (m/s)/(mJ/cm²) is the experimentally determined slope for the dependence of the primary melting front on fluence, F in mJ/cm² is the fluence, $E_{th} = 30$ mJ/cm² is the experimentally determined melting threshold, and t in ns is the time at which the primary melt front reaches its maximum depth.